Doctor of Philosophy

Photothermal-mediated Local Heating Using a Nano-Functionalized Stent to Suppress Stent-induced Tissue Hyperplasia in the Rat Gastric Outlet

The Graduate School
of the University of Ulsan

Department of Medicine
Min Tae Kim

Photothermal-mediated Local Heating Using a Nano-Functionalized Stent to Suppress Stent-induced Tissue Hyperplasia in the Rat Gastric Outlet

Supervisor: Ho-Young Song, Namkug Kim

A Dissertation

Submitted to
the Graduate School of the University of Ulsan
In partial Fulfillment of the Requirements
for the Degree of

Doctor of Philosophy

by

Min Tae Kim

Department of Medicine
Ulsan, Korea
August 2018

Photothermal-mediated Local Heating Using a Nano-Functionalized Stent to Suppress Stent-induced Tissue Hyperplasia in the Rat Gastric Outlet

This certifies that the dissertation
Of Min Tae Kim is approved.

Committee Chair Dr. Jae Yong Jeon

Committee Member Dr. Jin Hyoung Kim

Committee Member Dr. Tae-Hyung Kim

Committee Member Dr. Namkug Kim

Committee Member Dr. Ho-Young Song

Department of Medicine
Ulsan, Korea
August 2018

ACKNOWLEDGEMENT

부족한 제가 연구자의 길을 걸을 수 있도록 이끌어주신 존경하는 송호영 교수님, 어려움이 있을 때마다 아낌없는 조언으로 격려해주신 김남국 교수님께 진심으로 감사드립니다. 두 지도교수님의 훌륭한 가르침 덕분에 포기하지 않고 연구에 정진할 수 있었습니다. 앞으로도 두 분의 명성에 누가 되지 않도록 끊임없이 노력하는 연구자가 되겠습니다.

그리고 바쁘신 와중에 귀한 시간 내주셔서 논문 심사를 맡아주신 전재용, 김태형, 김진형 교수님께 깊은 감사의 말씀을 드립니다. 여러 교수님들의 조언덕분에 미진했던 부분을 수정/보완하여 완성도를 크게 높일 수 있었습니다. 교수님들의 은혜를 잊지 않겠습니다.

본 학위 논문 연구에 많은 도움을 주신 박정훈, 김건영, 조영철 선생님께도 감사의 말씀을 전합니다. 박정훈선생님의 많은 도움덕에 여기까지 올 수 있었던 것 같습니다. 많은 도움과 배움을 받아 이 자리를 빌어 깊은 감사의 마음을 전합니다. Dr. Jiaywei Tsauo and Nader gamal, thank you for your comments of my thesis. 하나의 연구실 공간에서 생활하면서 많은 분들의 도움으로 이 자리까지 올 수 있었던 것 같습니다. 앞으로 좋은일만 함께 하기를 기원합니다.

대학병원 방사선사로 근무하면서 학업을 병행하던 시절, 연구자가 되고 싶다는 확실한 꿈을 가지고 있었음에도 불구하고 일과 학업을 병행하는 것은 결코 쉽지 않았습니다. 제 스스로의 한계에 부딪힐 때마다 좌절하기도 했습니다. 그때마다 포기하지 않도록 버팀목이 되어주신 조재환 교수님, 고민이 있을 때마다 자신의 일처럼 생각해주시고 애정 어린 조언을 해주신 허영철 교수님 감사합니다. 두 분을 통해 제 인생의 방향을 잡고 성장할 수 있었습니다. 저도 언젠가 후배, 제자들에게 두 분과 같은 멘토가 되고 싶다는 꿈을 감히 가져봅니다.

학부과정 때부터 지켜봐주시고 격려해주신 고신관 교수님, 한동균 교수님께도 감사의 말씀 전합니다. 또 언제나 부족한 후배임에도 불구하고 좋게 봐주시고 챙겨주시는 홍주완 교수님, 박영준 교수님, 이진혁 선생님 감사합니다.

무엇보다 지금의 저를 있게 한 사랑하는 가족들. 오랫동안 공부하는 아들 믿고 지켜봐주신 아버지, 어머니 그리고 부족한 사위 항상 예뻐해 주시는 장모님 모두 감사하고 사랑합니다. 민수 형과 하나형수, 유진 누님과 영주 형님께도 감사드립

니다. 특히 저의 고민을 함께 해주고 조언해 준 처형에게 큰 감사의 말씀 전합니다.

마지막으로 나의 아내, 임서현에게 감사의 마음을 바칩니다. 힘들었던 그리고 좋았던 모든 찰나의 순간들을 당신과 함께할 수 있어 행복했습니다. 지금 이 순간에도, 앞으로도 모든 순간들을 함께하고 싶습니다. 고맙고 사랑합니다.

ABSTRACT

Background and Purpose: Despite advances in various stent technologies used to suppress stent-induced tissue hyperplasia, the current therapeutic strategies are insufficient. The purpose of this study is to investigate the effects of photothermal (PT)-mediated local heating on suppressing stent-induced tissue hyperplasia in the rat gastric outlet.

Materials and Methods: A branched gold nanoparticles (BGNPs)-coated, self-expandable metallic stent (SEMS) was produced through a two-step synthesis process in order to create a stent capable of PT-mediated local heating under near infrared (NIR) laser irradiation. Forty-five rats subjected to SEMS placement in the rat gastric outlet were randomly divided into three groups of 15 rats each. Group A received non-coated SEMS. Group B received BGNP-coated SEMS with local heating at 55 °C after SEMS placement. Group C received BGNP-coated SEMS without local heating. The therapeutic effectiveness of local heating was assessed by comparing the results of western blot analysis and histopathological analysis among the three groups. All groups of five each were immediately sacrificed after local heating for western blot analysis. HSP70 expression was assessed by western blot analysis. In addition, all groups of 10 each were sacrificed by administrating inhalable pure dioxide at four weeks after stent placement for histopathological analysis.

Results: BGNP-coated SEMSs were successfully fabricated using a two-step synthesis process. Stent placement and local heating were successful in all rats. Stent-induced tissue hyperplasia-related variables were significantly lower in group B than in groups A and C (all p <0.001). The mean degrees of CD31-positive-deposition were significantly lower in group B than in groups A and C ($p < 0.001$). However, the mean degrees of TUNEL-positive-deposition were significantly higher in group B than in groups A and C ($p < 0.001$). The Ki67-positive mesothelial monolayers were more prominent in groups A and C than in group B.

Conclusion: PT-mediated local heating suppresses tissue hyperplasia after stent placement in the rat gastric outlet.

(**Key words**: Photothermal therapy, Local heating, Gold nanoparticle, Stent-induced tissue hyperplasia, Gastric outlet obstruction)

CONTENTS

LIST OF FIGURES

LIST OF TABLES

LIST OF ABBREVIATIONS

PT	photothermal
BGNP	branched gold nanoparticle
SEMS	self-expandable metallic stent
NIR	near infra-red
GOO	gastric outlet obstruction
HSP	heat shock protein
GNP	gold nanoparticle
BPEI	branched polyethylenimine
PDA	polydopamine
DW	deionized water
PEI	polyethylenimine
SEM	scanning electron microscopy
EDS	energy-dispersive X-ray spectroscopy
IR	infra red
SD	**s**prague-dawley
IHC	immunohistochemistry
IF	immunofluorescence
PTT	photothermal therapy

INTRODUCTION

Placement of a self-expandable metallic stent (SEMS) has generally been used for palliation of unresectable, malignant gastric outlet obstructions (GOOs) (1-6). The SEMS was originally developed for treating malignant obstruction of the esophagus, colon, and gastric outlet. This treatment option reported favorable results comparable to those of surgery for palliation and as a bridge to surgery (7-10). Temporary SEMS placement for frequently recurrent benign GOO after serial dilations is also recommended (9, 11-16). However, these therapeutic options are restricted by stent-induced tissue hyperplasia that occurs in the uncovered portion of the SEMS or in both ends of the covered SEMS, and which can induce additional stricture with recurrent obstructive symptoms and increased technical failure of stent removal (9, 11). The downside of this SEMS placement for benign and malignant gastric outlet obstruction is restenosis resulting from tissue hyperplasia through the mesh or around the edges of the stents. With regard to tissue hyperplasia, a cause of stent obstruction induced by the SEMS itself, various substances such as dexamethasone, paclitaxel, sirolimus, a transforming growth factor beta inhibitor, and irradiation have been investigated in vitro and in vivo in order to prevent tissue hyperplasia after SEMS placement in various nonvascular, luminal organs (17-24). Unfortunately, current therapeutic strategies are insufficient for suppressing tissue hyperplasia in clinical trials.

Controlled local heat treatments have been introduced for cancer therapy and managing of tissue hyperplasia (25-27). It has been demonstrated that moderate heat (43–50°C) treatments can not only decrease in-stent restenosis caused by neointimal hyperplasia in animal artery models (27-29), but can also inhibit tissue hyperplasia with minimal damage to surrounding structures in rat skin (26). Local application of moderate temperatures reduces collagen accumulation, increases cell apoptosis, alters cell metabolism, and activates a family of heat shock proteins (HSPs) (26, 27). Thermal therapy using various

nanoparticles, such as different shaped gold nanoparticles (GNPs) and magnetic nanoparticles, has been extensively studied for inducing controlled heat treatments with high efficiency and accuracy (30, 31).

Over the last decade, various GNP-based agents with multifunctionality and high photothermal (PT)-converting efficiency have been investigated for biomedical applications to target diseases (31-34). Recently, Kim et al. reported a new type of branched GNP (BGNP) for highly efficient near infra-red (NIR) PT transducers (35). The synthesized BGNP showed distinct heating efficiency compared with conventional spherical GNPs. Our previous dose-range study using BGNP-coated SEMS with NIR irradiation demonstrated that moderate temperatures (50 to 65 °C) have a favorable effect regarding suppression of stent-induced tissue hyperplasia compared with a high temperature (80 °C) (27). However, this study did not provide the exact influence ranges of the localized, heated BGNP-coated SEMS and did not measure the exact temperature in an in vivo study (27). The temperature may be relatively reduced due to the cooling effects of blood flow compared to that seen in the in vitro results. In our study, newly developed nano-functionalized stents were required to be tested in vitro and simultaneously directly introduced to pre-clinical practice. We hypothesized that the temperature in vivo can be provided through the newly developed, rat gastric outlet model during local heating using a thermal camera as well as that this therapeutic strategy may also suppress stent-induced tissue hyperplasia by thermal-induced apoptosis and cell cycle arrest. Therefore, the purpose of this study is to investigate the effects of photothermal (PT)-mediated local heating on suppressing stent-induced tissue hyperplasia in the rat gastric outlet.

MATERIALS AND METHODS

Preparation of SEMSs

The SEMS was knitted from a single thread of 0.127-mm-thick nitinol wire filament (S&G biotech, Seongnam, Korea). The stent was 5 mm in diameter and 8 mm in length. Two radiopaque markers at each end of the stent facilitated precise placement. The gastroduodenal stent introducer set consisted of a 6-Fr sheath, a dilator, and a pusher catheter (Cook, Bloomington, IN, USA).

Fabrication of BGNP-coated SEMS

Branched polyethyleneimine (bPEI, M_w; 600 Da), dopamine hydrochloride, hydrogen tetrachloroaurate (III) trihydrate ($HAuCl_4$, 99.9%), silver nitrate ($AgNO_3$, 99%), L-ascorbic acid (≥98%), sodium borohydrate (98%) and sodium deoxycholate (≥97%) were used as purchased from Sigma–Aldrich (St. Louis, MO, USA).

The cationic polymer was coated on the surface of SEMS through polydopamine (PDA) coating prior to deposition of BGNPs on the surface. Dopamine hydrochloride (1 mg/mL) was dissolved in 15 mL of 5 mM Tris buffer (pH 8.5) and the stent was immersed in the dopamine solution. The coating process was carried out at room temperature with magnetic stirring for 12 h. The stent coated with PDA was washed with deionized water (DW), and the PDA coating process was repeated two additional times under the same conditions. Next, to coat the surface of the PDA-coated stent with a cationic polymer, the as-prepared PDA-coated stent was immersed in 15 mL of polyethyleneimine (PEI, 600 Da) solution (10 mg/mL) and was stirred at room temperature for 12 h. Finally, the PEI-coated stent was washed with DW. BGNPs were coated on the surface of a PEI-coated stent following a modified procedure detailed in our previous report.[21] The PEI-coated stent was immersed in 15 mL of 0.5 mM sodium cholate solution. Next, 90 μL of 50 mM $AgNO_3$, 3 mL of 10 mM $HAuCl_4$ solution, and 0.96 mL of 100 mM ascorbic acid solution were sequentially added to the solution containing the PEI-coated stent. The reaction allowed coating proceeding at room temperature for 12 h. The solution color after the reaction was dark purple. After the reaction, the BGNP-coated stent was washed with DW and dried at room temperature for 24 h (Fig. 1).

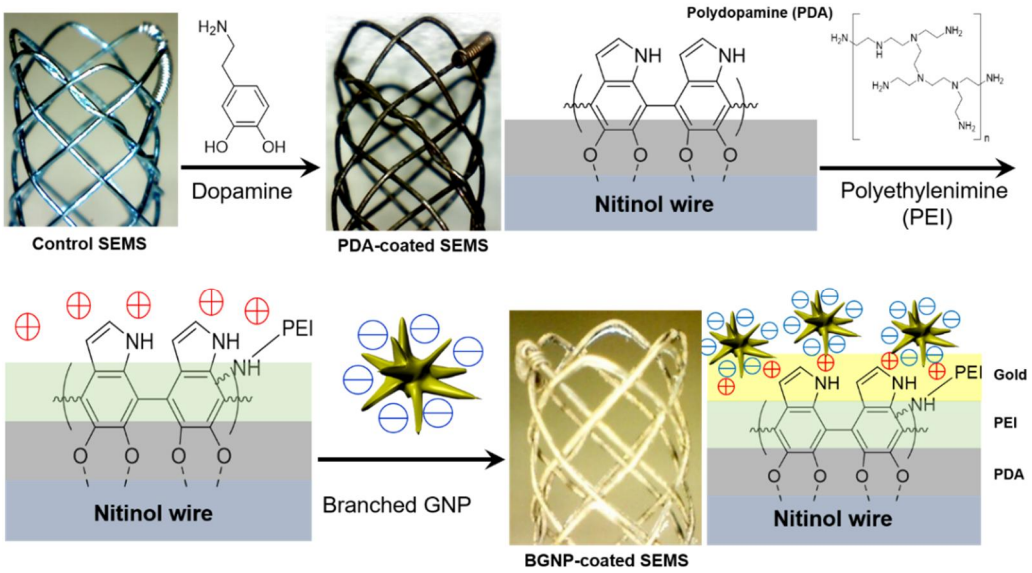

Figure 1. Schematic illustration of the preparation process for BGNP-coated SEMS: The cationic polymer was coated on the surface of SEMS through PDA-coating, and BGNPs were sequentially deposited on the polymer layer. Note. SEMS: self-expandable metallic stents; PDA: polydopamine; PEI: polyethylenimine; BGNP: branched gold nanoparticles.

Characterization of BGNP-coated SEMS

The surface characteristics of control, PDA-coated, and BGNP-coated SEMSs were examined by scanning electron microscopy (SEM, Philips XL-30, USA) with energy-dispersive X-ray spectroscopy (EDS, INCAx-sight, Oxford Instruments, Abingdon, Oxfordshire, UK). The three SEMSs were fixed on an aluminum pin stub through a carbon tape and then the surface was analyzed for elemental mapping of gold.

NIR laser induced photothermal properties *in vitro*

To investigate PT characteristics in vitro, the Control, PDA-coated, and BGNP-coated SEMSs were irradiated with a 1-mm diameter. fiber-coupled NIR (808 nm) diode-laser (OCLATM LASER, NDLUX Inc., Anyang, Korea) at 1.27 W/cm2. The irradiation was applied for 60 seconds. As the temperature increased, thermal images of the SEMS were examined using an IR thermal camera (ICI9320P, Infrared Cameras Inc., Beaumont, TX, USA). The images were stored as electronic image files every five seconds for 70 seconds (including 10 seconds after irradiation). All of the studies were repeated ten times in order to determine the statistical reproducibility.

Animal study

This study was approved by the Committee for Animal Research at our institution and conformed to the US National Institutes of Health guidelines regarding the care and use of laboratory animals. A total of 45 Sprague-Dawley (SD) male rats (Orient Bio, Seongnam, Korea), each weighing 300-350 g at nine weeks of age, underwent SEMS placement into the gastric outlet. The rats were randomly divided into two groups using Random Allocation software (version 2.0; Microsoft, Seattle, WA, USA), except for non-coated SEMS placement group (Fig. 2): Group A (n = 15) received non-coated SEMS and Group B (n = 15) received BGNP-coated SEMS with local heating at 55 ℃ after SEMS placement. Group C (n = 15) received BGNP-coated SEMS without local heating. Local heating was performed one week after stent placement. All of the groups of five each were sacrificed for western blot analysis immediately after local heating. In addition, all of the groups of 10 each were sacrificed by administrating inhalable pure dioxide four weeks after stent placement for histopathological analysis, respectively. The body weights of the rats were measured weekly until the sacrifice. The animals were housed one per cage in a room with 12-hour light and dark cycles at an environmental temperature (24 ± 1 ℃) and moisture (55 ± 10 %) and were provided standard rodent chow and water ad libitum. All of the animals were acclimatized for at least one week before the experimental session.

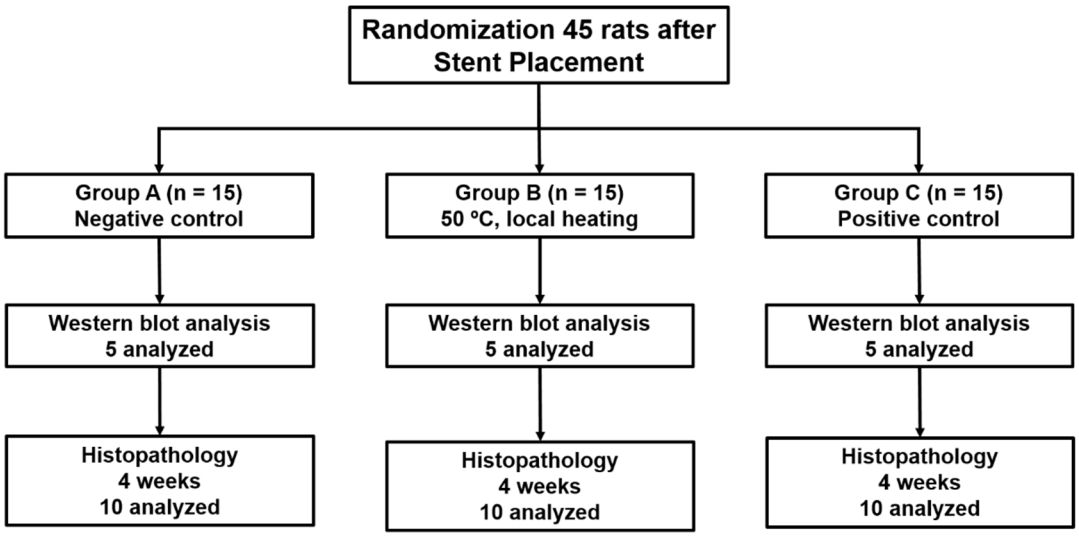

Figure 2. A flow diagram showing the randomization process and study follow-up.

Stent placement and PT-mediated local heating

Anesthesia was induced by intramuscular injection of 50 mg/kg zolazepam, 50 mg/kg tiletamine (Zoletil 50; Virbac, Carros, France), and 10 mg/kg xylazine (Rompun; Bayer HealthCare, Leverkusen, Germany). After overnight fasting, the procedure time was limited to less than 10 minutes for each animal in order to minimize the effect of room air tissue drying and the risk of infection, and all procedures were performed on a heating mat warmed to 38 °C while in a supine position.

The animals' abdomens were shaved with an electric clipper and the incision field was disinfected with 10% povidone-iodine and draped with sterile towels. A midline incision of the skin over a length of 5 cm was then made, and the musculoperitoneal layer was incised with a scalpel and opened using surgical scissors over a length of 5 cm along the linea alba. The middle portion of the anterior wall of the stomach body was grasped with forceps, after which a 0.5 cm-long incision was made at a right angle to the long axis of the stomach. A 30-cm microguide wire (Transend; Boston Scientific/Medi-Tech, Watertown, MA, USA) was introduced through the incision site of the stomach into the duodenum under fluoroscopic guidance (Artis Zee Multipurpose; Siemens, Muenchen, Germany). A 6-Fr sheath with a dilator (Cook, Bloomington, IN, USA) was introduced over the guide wire across the stomach until the distal tip of the stent tube reached the gastric outlet. With the sheath left in place, the dilator and the guide wire were removed. A stent in a compressed state was then loaded in the sheath and positioned in the gastric outlet with the use of a pusher catheter. The stent was deployed in the gastric outlet by withdrawing the sheath as the pusher catheter was held in place (Fig. 3 a, b). The sheath and the pusher catheter were pulled out of the stomach after stent placement. Suturing between the placed stent and the proximal end of the stent outlet was performed in order to prevent stent migration. The incision site of the stomach, peritoneum, and skin were sequentially closed with sutures.

PT-mediated local heating was performed one week after stent placement in the same gastrostomy manner. A guide wire was introduced through the gastrostomy into the duodenum under fluoroscopic guidance. A 6-Fr sheath was pass over the guide wire into the stomach and advanced until it reached the stented gastric outlet. For NIR laser irradiation, a 1-mm–diameter, fiber coupled NIR (808 nm) diode-laser (OCLA^{TM} LASER, NDLUX Inc., Anyang, Korea) was inserted into a 6-Fr sheath with a radiopaque tip so as to allow visualization under fluoroscopic guidance. The 6-Fr sheath with fiber coupled NIR diode-laser was inserted through the incision site of the stomach and advanced until the middle portion of the stented gastric outlet (Fig. 3c). NIR laser irradiation was applied for 60 s in group B. The temperature changes and thermal images were examined using an IR thermal camera. In groups A and C, the rats underwent the same procedure without PT-mediated local heating. After stent placement and local heating, all animals received an intramuscular injection of 0.05 mg/kg buprenorphine (Renophan; Hanlim Pharmaceutical, Seoul, Korea) every six hours for 48 hours in order to monitor pain control, and they were monitored until they recovered from the anesthesia and were then returned to their cages. No antibiotics were injected before, during or after the stent placement or local heating.

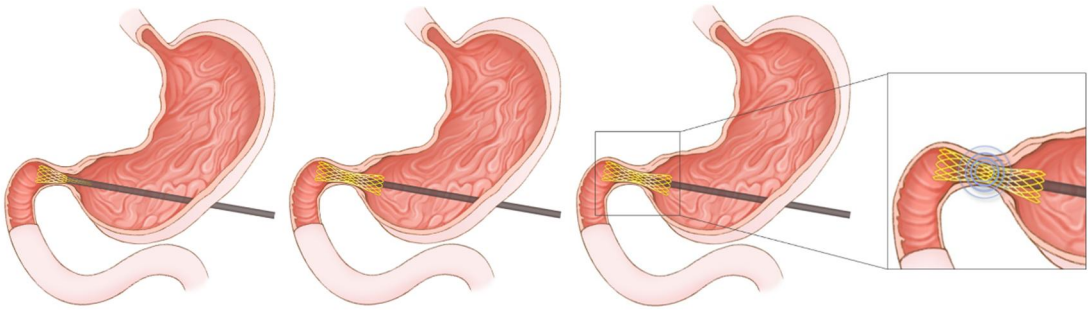

(a) **(b)** **(c)**

Figure 3. Schematic images show (a, b) the technical steps of stent placement and (c) photothermal-mediated local heating using a BGNP-coated SEMS.

Note. BGNP: branched gold nanoparticle; SEMS: self-expandable metallic stent

Western blot analysis

In order to confirm the PT-mediated, local heating effect of the BGNP-coated SEMS, the stented gastric outlet segments were collected seven days after local heating in all groups of rats of five each, respectively. Three, age-matched, healthy SD male rats (Orient Bio) maintained under the same conditions were used for presenting normal values of the gastric outlet. The HSP-70 (HSP-70, 1:1000; Abcam) antibody was used to compare the HSP70 expression between the groups. The membranes were incubated in secondary antibodies (1:10000; Jackson ImmunoResearch Laboratories, West Grove, PA, USA) conjugated to horseradish peroxidase (HRP). Target proteins were detected using ECL western blotting detection reagents (Amersham Biosciences, Little Chalfont, Buckinghamshire, England), and antigen-antibody complexes were visualized using an Ez-Capture MG software (ATTO Corporation, Tokyo, Japan). CS analyzer software (ATTO Corporation) was used to quantify the bands, and the data are expressed as the ratio of band intensity to that of β-actin.

Histological analysis

Surgical exploration of the entire duodenum and stomach was followed by gross examination in order to determine possible duodenal injury after stent placement or irradiation. Tissue samples were fixed in 10% neutral buffered formalin for 24 h, and which was then embedded in paraffin and sectioned. The stented gastric outlet was sectioned transversely in the proximal, middle, and distal regions. The slides were stained with hematoxylin and eosin (H&E) and Masson's Trichrome (MT). Histological evaluation using H&E included determining the granulation tissue-related percentage of the gastric outlet cross-sectional area of stenosis calculated as 100 × (1 - [stenotic stented area/original stented area]) (18, 19). The degree of collagen deposition and the percentage of connective tissue area were determined using MT-stained sections. The connective tissue (collagen) area was calculated as follows: 100 × (1 - [connective area/original area]). The level of collagen deposition was subjectively determined, where 1 = mild, 2 = mild to moderate, 3 = moderate, 4 = moderate to severe, and 5 = severe. Histological analysis of the gastric outlet was performed using a BX51 microscope (Olympus, Tokyo, Japan). Image-Pro Plus software (Media Cybernetics, Silver Spring, MD, USA) was used for measurements. The analyses of the histological findings were accessed on the basis of the consensus of three observers blinded to their group assignment.

Immunohistochemical analysis

Immunohistochemistry (IHC) was performed on paraffin-embedded transverse sections of stented duodenum with TUNEL (Apoptotag kit, Biogene, Darmstadt, Germany), CD31 (rabbit polyclonal IgG, 1:200; Abcam, Cambridge, UK), and as the primary antibodies. The sections were visualized with a BenchMark XT IHC automated immunohistochemical stainer (Ventana Medical Systems, Tucson, AZ, USA). TUNEL and the CD31-positive-deposition degree were subjectively determined where 1 = mild, 2 = mild to moderate, 3 = moderate, 4 = moderate to severe, and 5 = severe. IHC findings were obtained on the basis of the consensus of three observers blinded to the study.

Immunofluorescence analysis

The stented gastric outlet was harvested and fixed by immersion in 4% paraformaldehyde containing perfusion buffer at 4°C, and followed by sequential incubation in 15% and 30% sucrose solution. The well-fixed samples were then embedded in the optimal cutting temperature compound, and 6-um cryostat sections were prepared and collected on slides for the subsequent staining steps. Immunofluorescence (IF) staining was performed using Ki67. Slides were acquired with 3D-Histech Mirax scanner (3D HISTECH, Budapest, Hungary).

Statistical analysis

The temperatures on the *in vitro* and *in vivo* were analyzed using the Wilcoxon signed-rank test. Differences between the groups were analyzed using the Kruskal–Wallis or Mann–Whitney U test, as appropriate. A p value of < 0.05 was considered statistically significant. Statistical analyses were performed using SPSS software (version 23.0; SPSS, IBM, Chicago, IL, USA).

RESULTS

Characterization of BGNP-coated SEMS

BGNP-coated SEMSs were successfully fabricated using a two-step synthesis process. Elemental analysis (Fig. 4 a-c) revealed that nickel (blue) and titanium (green) signals were predominantly detected in the SEMS composed of nitinol wires. In the PDA-coated SEMS, the signal for carbon (pink) increased compared to that in the control SEMS. The signal for gold (red) was significantly increased in the BGNP-coated SEMS.

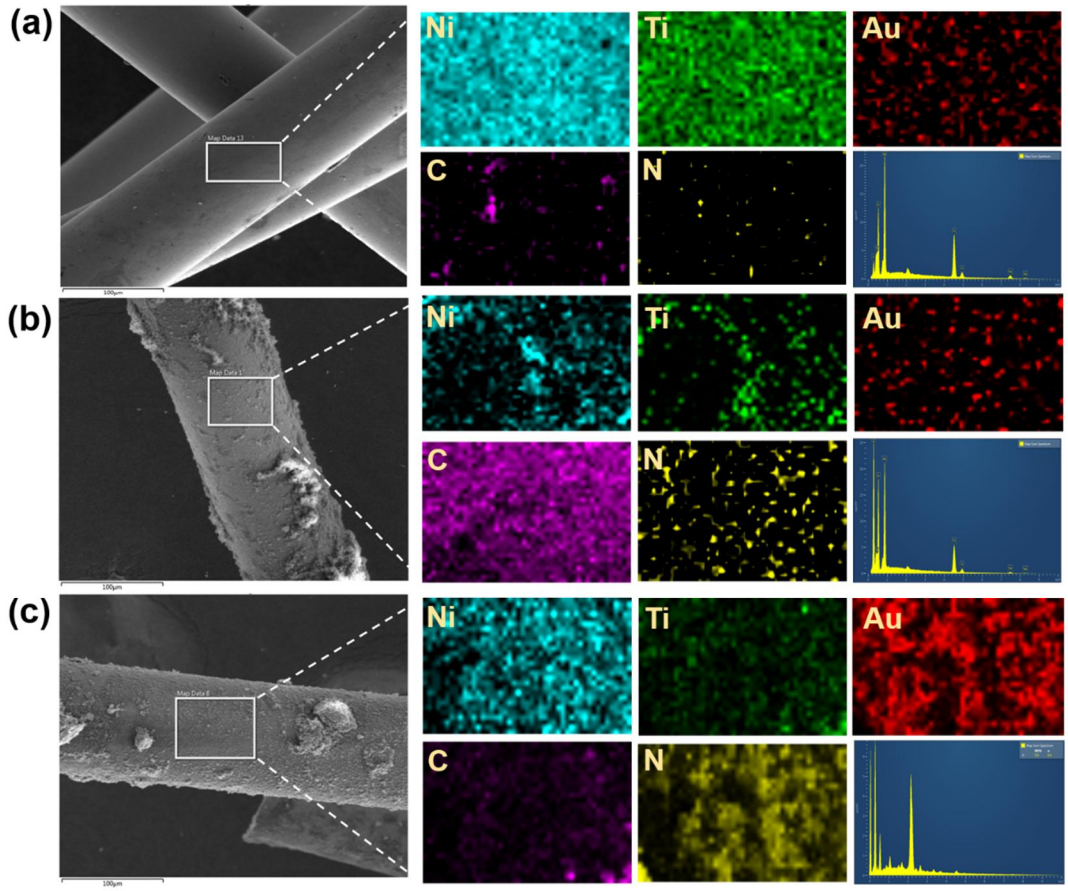

Figure 4. SEM and EDS mapping analysis of SEMS (a) nitinol SEMS, (b) PDA-coated SEMS, and (c) BGNP-coated SEMS (blue, green, red, pink, and yellow colors indicate nitinol, titanium, gold, carbon, and nitrogen, respectively).

Note. PDA, polydopamine; BGNP, branched gold nanoparticles; SEMS, self-expandable metallic stents; SEM, scanning electron microscopy; EDS, energy dispersive spectroscopy.

Photothermal properties of *in vitro* and *in vivo*

In the *in vitro* study, the stent surface temperature reached steady-state plateau values by 60 seconds upon NIR irradiation and then rapidly cooled after cessation of irradiation (Fig. 5). The mean steady-state surface temperature (± standard deviation [SD]) of the control, PDA-coated, and BGNP-coated SEMS samples were 40.01 (± 0.56), 46.24 (± 0.27), and 55.18 (± 0.64) °C, respectively, under NIR laser irradiation at 1.27 W/cm^2 (Fig. 5c).

The mean steady-state surface temperature (± SD) of the BGNP-coated SEMSs during PT-mediated local heating in the rat gastric outlet after stent placement was 49.22 (± 0.44) °C at 1.27 W/cm^2 (Fig. 5d). The mean temperature on the *in vivo* (49.22 °C) was significantly reduced compared with that on the *in vitro* (55.18 °C) with a 10.8% decrease ($p < 0.001$, Wilcoxon signed-rank test).

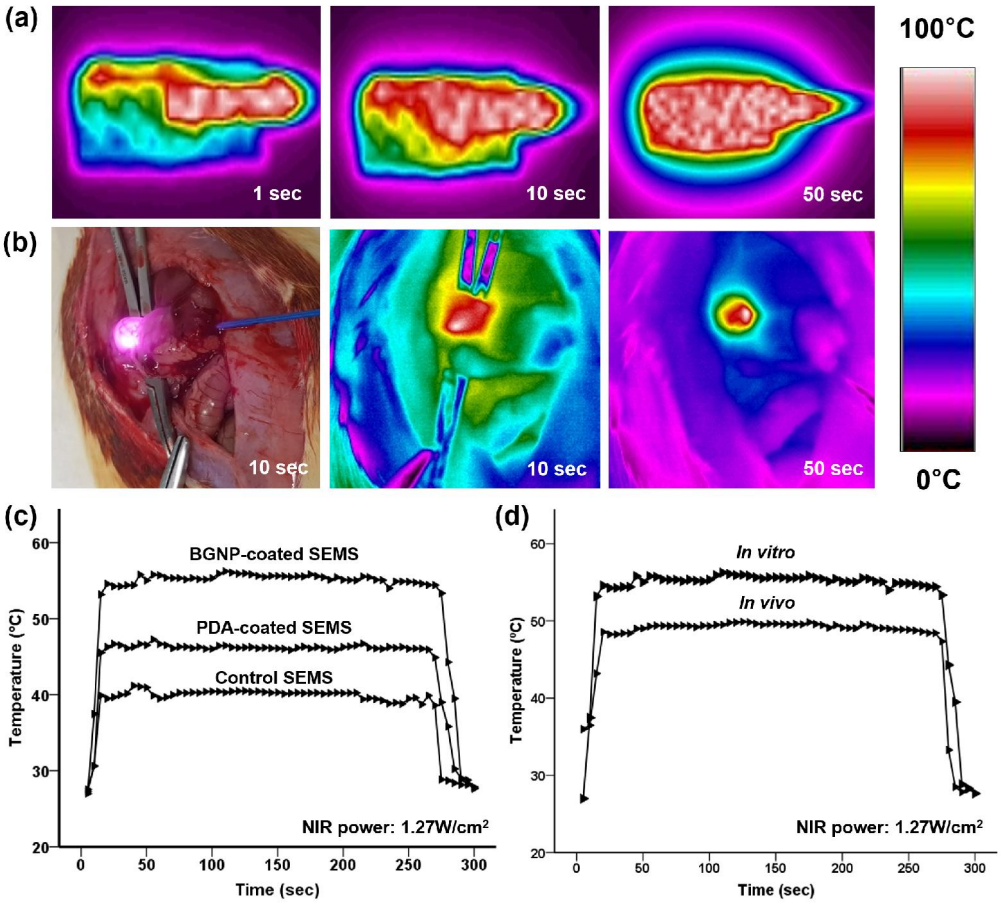

Figure 5. Infrared thermal camera images (a) in vitro and (b) in vivo and temperature change measurement of (c) control SEMS, PDA-coated SEMS, and BGNP-coated SEMS under irradiation with an 808-nm laser at 1.27 W/cm^2. (d) The graph shows the temperature difference of the stent under NIR laser irradiation at 1.27 W/cm^2 between *in vitro* and *in vivo* results.

Stent placement and PT-mediated local heating

Stent placement and PT-mediated local heating were technically successful in all rats with no procedure-related complications. There was no evidence of stent obstruction or stent migration in any of the rats, and all of the stents were fully expanded within one week. All of the rats survived until the end of the study. Stent placement and local heating procedures did not affect any of the rats in terms of their body weight and behavior. There were also no significant differences in body weight after stent placement between the groups ($p > 0.05$) (Table 1).

Table 1. Effects of stent placement and local heating procedures on body weight changes

Groups	Body weight (g, mean ± SD)					* Weight change (%)
	Before	Day 7	Day 14	Day 21	Day 28	
A	346.7±12.11	354.6±19.32	373.56±19.79	398.86±24.57	425.8±25.62	81.4
B	342.4±24.42	354.3±29.41	371.7±24.81	400.7±24.76	427.4±23.43	80.1
C	340.7±22.75	350.7±24.03	371.3±25.03	396.9±20.69	425±19.61	80.1

Note. SD: standard deviation, Kruskal–Wallis test.

Western blot findings

There was statistically difference in HSP 70 expression between the groups (p = 0.002, Kruskal-Wallis test). HSP 70 expression was significantly higher in group B than in groups A and C (A vs B, p = 0.002; B vs C, p = 0.002, Mann–Whitney U test), although there were no significant differences between groups A and C (p = 0.543, Mann–Whitney U test) (Fig. 6).

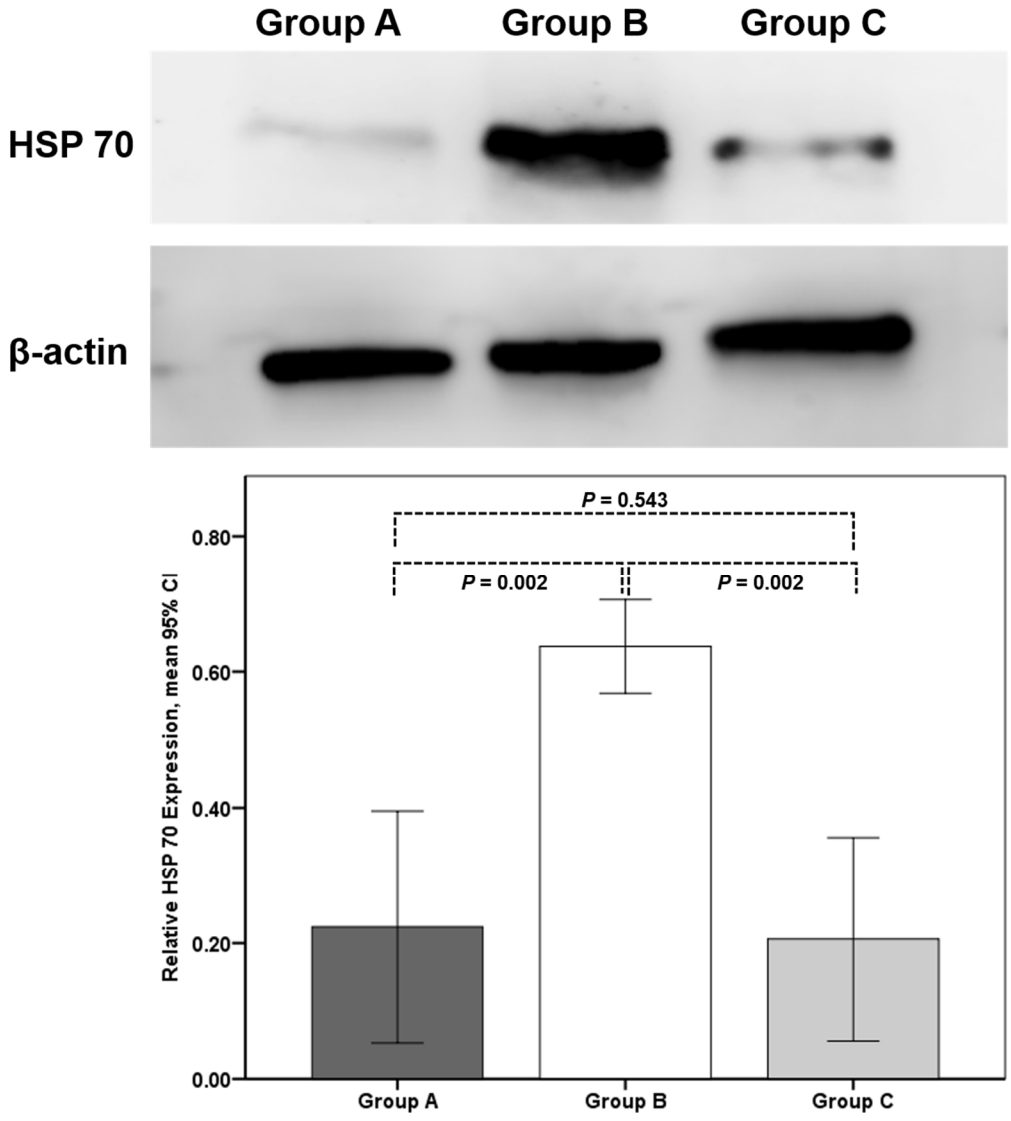

Figure 6. Expression level of heat shock protein 70 (HSP70). (a) Representative expression of HSP70 and (b) relative fold induction of HSP70 expression levels. β-Actin was used as a reference.

Histological, histochemical findings

The histological findings are summarized in Table 2 and representative examples are shown in Figures 7 and 8. The mean percentage of the granulation tissue area, the mean percentage of the connective tissue area, the mean degree of the collagen deposition, and the mean degree of the TUNEL, CD31-positive deposition differed significantly in the groups (all variables; $p < 0.001$, Kruskal-Wallis test).

The mean percentage of the granulation tissue area, the mean percentage of the connective tissue area, the mean degree of the collagen deposition, and CD31 were significantly lower in group B than in groups A and C (A vs. B and B vs. C; all $p < 0.05$, Mann–Whitney U test). However, the mean degrees of TUNEL-positive-deposition were significantly higher in group B than in groups A and C (all $p < 0.05$). However, there were no significant differences between groups A and C (A vs. C; $p > 0.005$). The Ki67-positive mesothelial monolayers were more prominent in groups A and C than in group B (Fig. 9).

Table 2. Histological and immunohistochemical findings after BGNP-coated stent placement with or without local heating

	Group A	Group B	Group C	* *p*-value	+ *p*-value (A vs. B)	+ *p*-value (A vs. C)	+ *p*-value (B vs. C)
Granulation-tissue-area percentage (%)	59.01±7.60	28.36±6.50	59.15±8.45	< 0.001	< 0.001	0.879	< 0.001
Connective-tissue-area percentage (%)	37.14±4.50	15.49±3.18	37.23±6.06	< 0.001	< 0.001	0.650	< 0.001
Collagen-deposition degree	3.5±0.52	1.50±0.52	3.70±0.48	< 0.001	< 0.001	0.480	< 0.001
TUNEL-positive degree	1.30±0.48	2.90±0.73	1.50±0.53	< 0.001	< 0.001	0.374	0.001
CD31-positive degree	3.5±0.52	2.00±0.47	3.70±0.75	< 0.001	< 0.001	0.480	< 0.001

Note. Data are presented as mean ± standard deviation. * Kruskal–Wallis test, + Mann–Whitney U test.

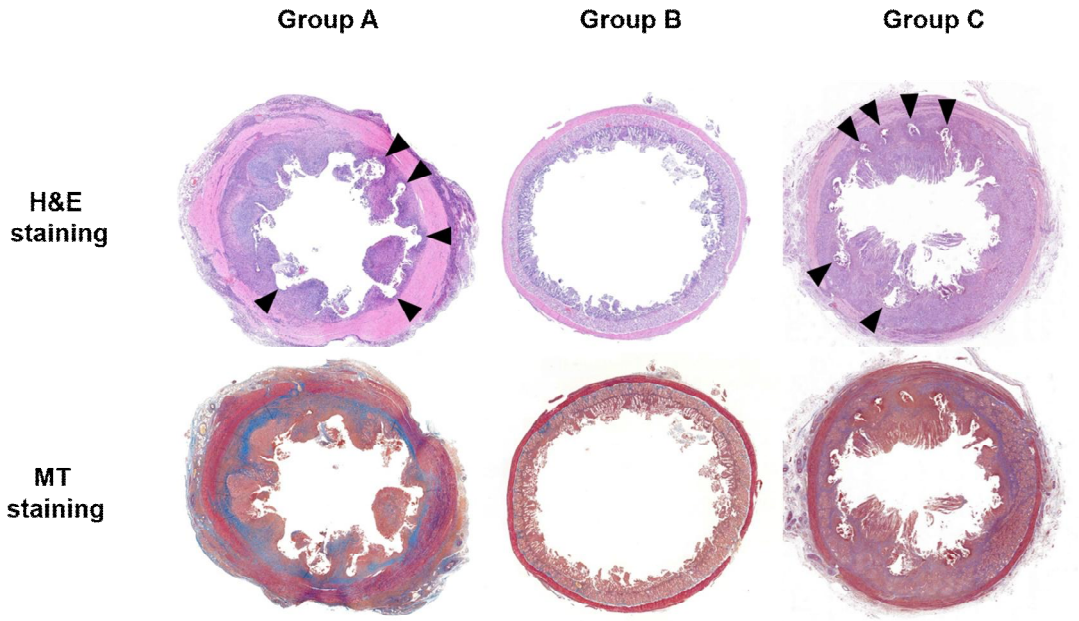

Figure 7. Representative microscopic images of histological sections obtained four weeks after stent placement. Hematoxylin and eosin (H&E) and Masson's trichrome (MT) of the groups. Arrowheads = stent struts (magnification ×1.25)

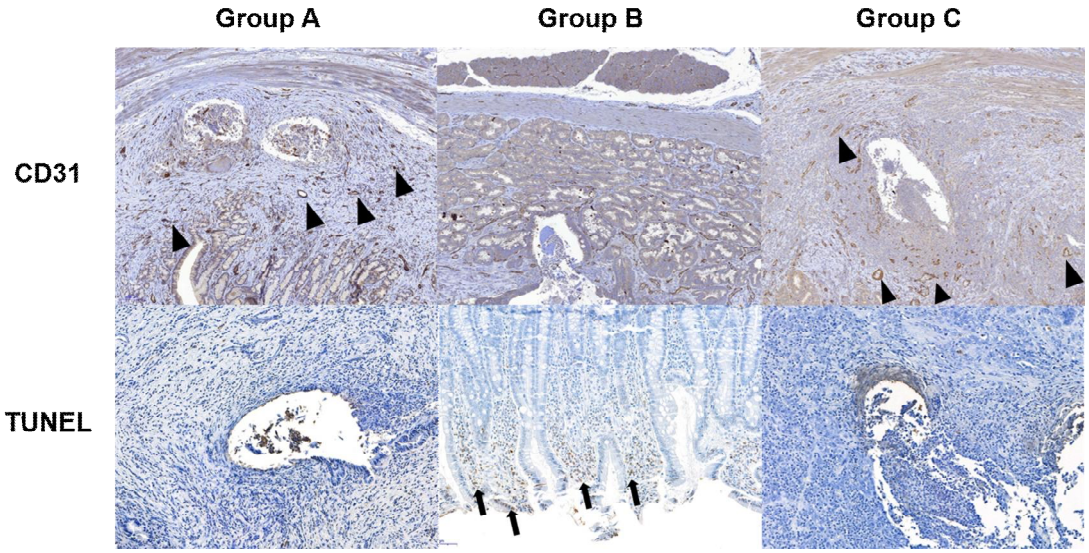

Figure 8. Representative microscopic images of immunohistochemistry sections obtained four weeks after stent placement. CD31 was significantly lower in the group B than in the groups A and C (Arrowheads = microvessels) (magnification ×10). TUNEL expressions were significantly higher in the group B than in groups A and C (Arrows = TUNEL-positive cells) (magnification ×10).

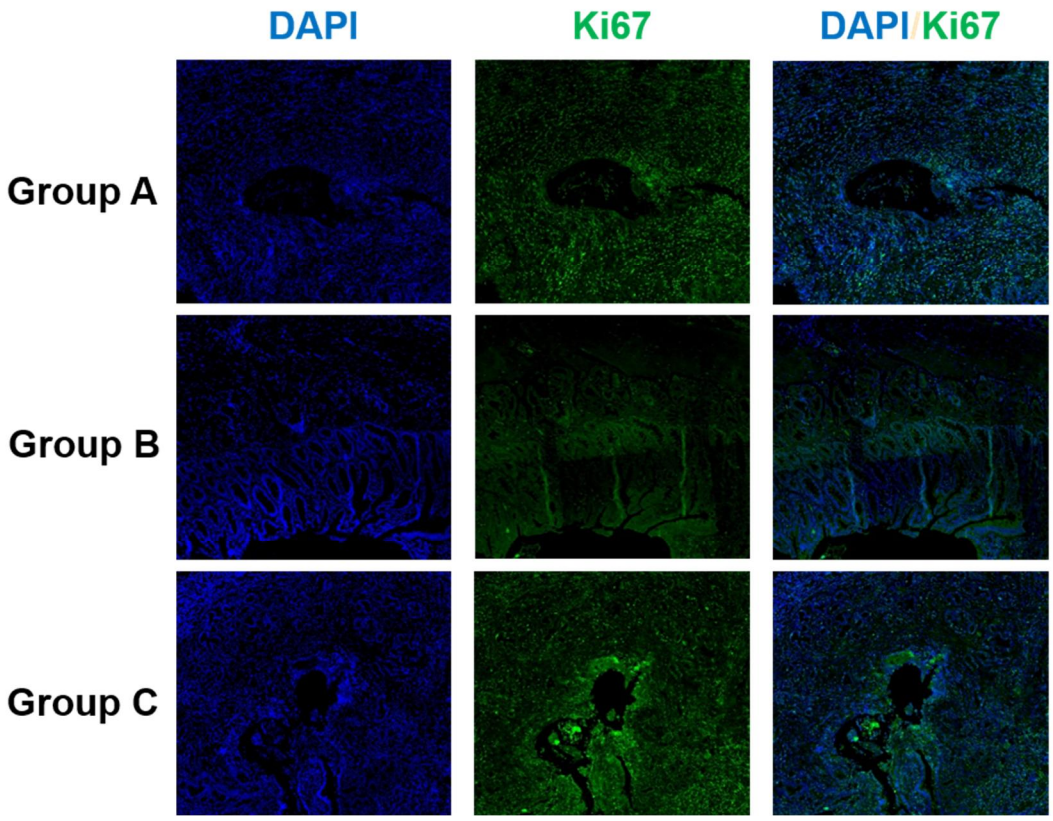

Figure 9. Representative immunofluorescence (DAPI = blue; Ki 67 = green) images show that the Ki 67-positive mesothelial monolayer was less prominent in the groups A and C than in the group B (magnification × 10).

DISCUSSION

In this study, we were able to successfully coat SEMSs with BGNPs which are known to generate significant heat when irradiated with an NIR laser. *In vitro*, the BGNP-coated SEMSs were successfully heated to therapeutic temperatures within several seconds of the NIR laser irradiation. Although the temperature at the stented rat gastric outlet was relatively reduced compared to the *in vitro* results, the stented gastric outlet was successfully heated, as evidenced by the significant increases in the HSP70 expression level. Tissue hyperplasia-related histopathological results were significantly decreased in group B compared to groups A and C. Apoptosis was significantly increased in the heated duodenal mucosa, and markers of cellular proliferation were significantly decreased after PT-mediated local heating, when compared to the non-heated groups. Increases in HSP expression and thermal induced-apoptosis are well-characterized features of the heat shock response, and previous studies have reported that HSP70 is an indicator of heat stress in different species (36, 37). In addition, a reduction of microvessel density showed that stent-induced tissue hyperplasia is associated with re-vascularization and re-epithelialization (38-40). Taken together, our results demonstrated that PT-mediated local heating via BGNP-coated SEMS using NIR laser irradiation successfully suppressed stent-induced tissue hyperplasia secondary to SEMS placement in the rat gastric outlet.

The BGNP-coated SEMS for PT-mediated therapy was synthesized by a facile, two-step process. The surface of the control SEMS was first modified using PDA (41), which helps BGNPs adhere to the surface of the nitinol stent, after which BGNPs were then attached to the PDA-coated surface of the stent. The SEM results showed that the BGNPs were uniformly coated through electrostatic interactions with the PDA-mediated cationic polymer coating layer. Surface modification of the stent with nanoparticles is important for inducing PT effects under physiological conditions. To confirm the PT effects, the BGNP-coated SEMS was irradiated using an NIR laser, and the change in temperature was observed using a thermal imaging camera. The BGNP-coated SEMS rapidly reached relatively a high temperature compared to the control and PDA-coated SEMSs. The temperature of the BGNP-coated SEMS was increased in proportion to the NIR intensity. These results indicate

that BGNP-coated SEMS shows excellent heat generation by NIR irradiation, and the PT properties can be easily controlled by adjusting the NIR irradiation power. This can be attributed to the anisotropic structural property of BGNP, and which is consistent with the results demonstrated in our previous report (35).

For optimal application of BGNP-coated SEMS in gastric outlet obstruction, BGNP-coated SEMS should be able to supply benign and malignant obstruction. Currently, a partially covered or completely covered SEMS was in use. Considering the possibility of major complications after SEMS placement, migration of the SEMS is one of the major complications (9, 42). The use of a dual stent increased the clinical outcomes, not only the technical and clinical success rates but also stent migration (9, 11, 42). Our study excluded the possibility of migration to assess the inhibition of stent-induced tissue hyperplasia. Another problem is that disruption of the covering membranes and the uncovered area of SEMS, both of which lead to tumor overgrowth and stent-induced tissue hyperplasia (11, 42). In order to prevent long-term complications, our study showed that adequate local heating of BGNP-coated SEMS could prevent stent-induced tissue hyperplasia in the rat gastric outlet. BGNP-coated SEMS may also be of potential value for preventing tumor ingrowth (43, 44). We hypothesized that PTT may prove to be effective in preventing or delaying the tumor ingrowth of a malignant gastric outlet obstruction in a rat. Further studies will be necessary in order to prove the effect of PTT.

Wound healing resulting from mechanical injury of the stent on the duodenal wall can be divided into at least three overlapping phases that occur over four weeks, i.e. inflammation, proliferation, and remodeling (45-47). The healing cascade immediately begins following mechanical injuries; the proliferative phase begins between days four and 14 and is characterized by increased fibroblasts, myofibroblasts, and angiogenesis with a decreasing inflammatory phase (38-40, 46, 47). During the proliferative phase, formation of the epithelium and re-vascularization occurs in order to cover the wound surface with concomitant tissue hyperplasia (45). PT-mediated local heating under NIR laser irradiation was performed seven days after stent placement to prevent stent-induced cell proliferation. There is no consensus regarding the optimal timing of local heating after stent-related tissue injuries. Although our heating strategy showed promising results, the ideal time for local

heating in order to prevent stent-induced tissue hyperplasia after stent placement remains controversial.

There were some limitations to our study. First, the results observed in this study may not reflect all of the pathological mechanisms occurring in humans. Second, it is necessary to determine the optimal timing for local heating in order to suppress stent-induced tissue hyperplasia. Third, we did not evaluate the depth penetration of the heated BGNP-coated SEMSs in the rat gastric outlet. Although additional studies will be required in order to determine the depth penetration of the heated BGNP-coated SEMS, our study supports the premise that PT-mediated local heating prevents stent-induced tissue hyperplasia after stent placement.

Advances in stent technology have resulted in low complication as well as high technical success rates, however, long-term preservation of stent patency remains technically challenging. Localized PT therapy may be valuable for preventing stent-induced tissue hyperplasia and tumor ingrowth and/or overgrowth after SEMS placement in patients with malignant and benign gastric outlet obstruction. An optic fiber for NIR laser irradiation may be easily delivered though the working channel of the endoscope after BGNP-coated SEMS placement. Under endoscopic visualization, controlled PTT can be applied to a region of interest. The excellent stability of the BGNP-coated SEMS and its therapeutic strategy will provide opportunities for clinical application in order to prevent in-stent restenosis in the gastrointestinal tract. However, further studies are warranted to determine its efficacy and safety as seen in preclinical trials. In conclusion, SEMS placement in the rat gastric outlet proved to be feasible and an efficient approach to stimulate stent-induced tissue hyperplasia as a potential model for reproducing the mechanisms of restenosis. In conclusion, PT-mediated local heating suppresses tissue hyperplasia after stent placement in the rat gastric outlet. Further preclinical studies will be required to investigate the efficacy and safety of PT-mediated local heating using BGNP-coated SEMS with NIR laser irradiation.

REFERENCES

1. van Halsema EE, Fockens P, van Hooft JE. 33 - Palliation of Gastric Outlet Obstruction A2 - Chandrasekhara, Vinay. In: Elmunzer BJ, Khashab MA, Muthusamy VR, editors. Clinical Gastrointestinal Endoscopy (Third Edition). Philadelphia: Content Repository Only!; 2019. p. 367-73.e2.

2. Lopera JE, Brazzini A, Gonzales A, Castaneda-Zuniga WR. Gastroduodenal stent placement: current status. Radiographics : a review publication of the Radiological Society of North America, Inc. 2004;24(6):1561-73.

3. van Hooft JE, van Montfoort ML, Jeurnink SM, Bruno MJ, Dijkgraaf MG, Siersema PD, et al. Safety and efficacy of a new non-foreshortening nitinol stent in malignant gastric outlet obstruction (DUONITI study): a prospective, multicenter study. Endoscopy. 2011;43(8):671-5.

4. Kim JH, Song HY, Shin JH, Choi E, Kim TW, Jung HY, et al. Metallic stent placement in the palliative treatment of malignant gastroduodenal obstructions: prospective evaluation of results and factors influencing outcome in 213 patients. Gastrointestinal endoscopy. 2007;66(2):256-64.

5. Park JH, Lee JH, Song HY, Choi KD, Ryu MH, Yun SC, et al. Over-the-wire versus through-the-scope stents for the palliation of malignant gastric outlet obstruction: A retrospective comparison study. Eur Radiol. 2016;26(12):4249-58.

6. Tringali A, Didden P, Repici A, Spaander M, Bourke MJ, Williams SJ, et al. Endoscopic treatment of malignant gastric and duodenal strictures: a prospective, multicenter study. Gastrointestinal endoscopy. 2014;79(1):66-75.

7. Hosono S, Ohtani H, Arimoto Y, Kanamiya Y. Endoscopic stenting versus surgical gastroenterostomy for palliation of malignant gastroduodenal obstruction: a meta-analysis. Journal of gastroenterology. 2007;42(4):283-90.

8. Sagar J. Colorectal stents for the management of malignant colonic obstructions. The Cochrane database of systematic reviews. 2011(11):Cd007378.

9. Heo J, Jung MK. Safety and efficacy of a partially covered self-expandable metal stent in benign pyloric obstruction. World J Gastroenterol. 2014;20(44):16721-5.

10. Bekheet N, Kim MT, Park JH, Kim KY, Tsauo J, Zhe W, et al. Fluoroscopic Gastroduodenal Stent Placement in 55 Patients with Endoscopic Stent Placement Failure. Cardiovasc Intervent Radiol. 2018.

11. Choi WJ, Park JJ, Park J, Lim EH, Joo MK, Yun JW, et al. Effects of the temporary placement of a self-expandable metallic stent in benign pyloric stenosis. Gut Liver. 2013;7(4):417-22.

12. Griffin SM, Chung SC, Leung JW, Li AK. Peptic pyloric stenosis treated by endoscopic balloon dilatation. Br J Surg. 1989;76(11):1147-8.

13. Lau JY, Chung SC, Sung JJ, Chan AC, Ng EK, Suen RC, et al. Through-the-scope balloon dilation for pyloric stenosis: long-term results. Gastrointest Endosc. 1996;43(2 Pt 1):98-101.

14. Misra SP, Dwivedi M. Long-term follow-up of patients undergoing ballon dilation for benign pyloric stenoses. Endoscopy. 1996;28(7):552-4.

15. Solt J, Bajor J, Szabo M, Horvath OP. Long-term results of balloon catheter dilation for benign gastric outlet stenosis. Endoscopy. 2003;35(6):490-5.

16. Benjamin SB, Cattau EL, Glass RL. Balloon dilation of the pylorus: therapy for gastric outlet obstruction. Gastrointest Endosc. 1982;28(4):253-4.

17. Han K, Park JH, Yang SG, Lee DH, Tsauo J, Kim KY, et al. EW-7197 eluting nano-fiber covered self-expandable metallic stent to prevent granulation tissue formation in a canine urethral model. PLoS One. 2018;13(2):e0192430.

18. Jun EJ, Park JH, Tsauo J, Yang SG, Kim DK, Kim KY, et al. EW-7197, an activin-like kinase 5 inhibitor, suppresses granulation tissue after stent placement in rat esophagus. Gastrointest Endosc. 2017;86(1):219-28.

19. Kim KY, Park JH, Kim DH, Tsauo J, Kim MT, Son WC, et al. Sirolimus-eluting Biodegradable Poly-l-Lactic Acid Stent to Suppress Granulation Tissue Formation in the Rat Urethra. Radiology. 2018;286(1):140-8.

20. Park JH, Song HY, Shin JH, Kim JH, Jun EJ, Cho YC, et al. Polydioxanone biodegradable stent placement in a canine urethral model: analysis of inflammatory reaction and biodegradation. Journal of vascular and interventional radiology : JVIR. 2014;25(8):1257-64.e1.

21. Park JH, Kim JH, Kim EY, Kim J, Song HY, Kim WJ, et al. Bioreducible polymer-delivered siRNA targeting MMP-9: suppression of granulation tissue formation after bare metallic stent placement in a rat urethral model. Radiology. 2014;271(1):87-95.

22. Farooq V, Serruys PW, Heo JH, Gogas BD, Onuma Y, Perkins LE, et al. Intracoronary optical coherence tomography and histology of overlapping everolimus-eluting bioresorbable vascular scaffolds in a porcine coronary artery model: the potential implications for clinical practice. JACC Cardiovascular interventions. 2013;6(5):523-32.

23. Kotsar A, Nieminen R, Isotalo T, Mikkonen J, Uurto I, Kellomaki M, et al. Biocompatibility of new drug-eluting biodegradable urethral stent materials. Urology. 2010;75(1):229-34.

24. Shin JH, Song HY, Choi CG, Yuk SH, Kim JS, Kim YM, et al. Tissue hyperplasia: influence of a paclitaxel-eluting covered stent--preliminary study in a canine urethral model. Radiology. 2005;234(2):438-44.

25. Chu KF, Dupuy DE. Thermal ablation of tumours: biological mechanisms and advances in therapy. Nat Rev Cancer. 2014;14(3):199-208.

26. Landsberg R, DeRowe A, Katzir A, Shtabsky A, Fliss DM, Gil Z. Laser-induced hyperthermia for treatment of granulation tissue growth in rats. Otolaryngol Head Neck Surg. 2009;140(4):480-6.

27. Brasselet C, Durand E, Addad F, Vitry F, Chatellier G, Demerens C, et al. Effect of local heating on restenosis and in-stent neointimal hyperplasia in the atherosclerotic rabbit model: a dose-ranging study. Eur Heart J. 2008;29(3):402-12.

28. Okada M, Hasebe N, Aizawa Y, Izawa K, Kawabe J, Kikuchi K. Thermal treatment attenuates neointimal thickening with enhanced expression of heat-shock protein 72 and suppression of oxidative stress. Circulation. 2004;109(14):1763-8.

29. Li L, Wang R, Shi HH, Xie L, Li JD, Kong WC, et al. In vitro study on the feasibility of magnetic stent hyperthermia for the treatment of cardiovascular restenosis. Exp Ther Med. 2013;6(2):347-54.

30. Huang X, El-Sayed IH, Qian W, El-Sayed MA. Cancer cell imaging and photothermal therapy in the near-infrared region by using gold nanorods. J Am Chem Soc. 2006;128(6):2115-20.

31. Cai W, Gao T, Hong H, Sun J. Applications of gold nanoparticles in cancer nanotechnology. Nanotechnol Sci Appl. 2008;1:17-32.

32. Ferrari M. Cancer nanotechnology: opportunities and challenges. Nat Rev Cancer. 2005;5(3):161-71.

33. Hirsch LR, Stafford RJ, Bankson JA, Sershen SR, Rivera B, Price RE, et al. Nanoshell-mediated near-infrared thermal therapy of tumors under magnetic resonance guidance. Proc Natl Acad Sci U S A. 2003;100(23):13549-54.

34. Park W, Cho S, Huang X, Larson AC, Kim DH. Branched Gold Nanoparticle Coating of Clostridium novyi-NT Spores for CT-Guided Intratumoral Injection. Small. 2017;13(5).

35. Kim DH, Larson AC. Deoxycholate bile acid directed synthesis of branched Au nanostructures for near infrared photothermal ablation. Biomaterials. 2015;56:154-64.

36. Kamanga-Sollo E, Pampusch MS, White ME, Hathaway MR, Dayton WR. Effects of heat stress on proliferation, protein turnover, and abundance of heat shock protein messenger ribonucleic acid in cultured porcine muscle satellite cells. Journal of animal science. 2011;89(11):3473-80.

37. Furusawa Y, Iizumi T, Fujiwara Y, Zhao QL, Tabuchi Y, Nomura T, et al. Inhibition of checkpoint kinase 1 abrogates G2/M checkpoint activation and promotes apoptosis under heat stress. Apoptosis : an international journal on programmed cell death. 2012;17(1):102-12.

38. Zhang M, Cresswell N, Tavora F, Mont E, Zhao Z, Burke A. In-stent restenosis is associated with neointimal angiogenesis and macrophage infiltrates. Pathology, research and practice. 2014;210(12):1026-30.

39. Arnold F, West DC. Angiogenesis in wound healing. Pharmacology & therapeutics. 1991;52(3):407-22.

40. Wu Y, Chen L, Scott PG, Tredget EE. Mesenchymal stem cells enhance wound healing through differentiation and angiogenesis. Stem cells (Dayton, Ohio). 2007;25(10):2648-59.

41. Lee H, Dellatore SM, Miller WM, Messersmith PB. Mussel-inspired surface chemistry for multifunctional coatings. Science (New York, NY). 2007;318(5849):426-30.

42. Song HY, Shin JH, Yoon CJ, Lee GH, Kim TW, Lee SK, et al. A dual expandable nitinol stent: experience in 102 patients with malignant gastroduodenal strictures. Journal of vascular and interventional radiology : JVIR. 2004;15(12):1443-9.

43. Zhao K, Cho S, Procissi D, Larson AC, Kim DH. Non-invasive monitoring of branched Au nanoparticle-mediated photothermal ablation. J Biomed Mater Res B Appl Biomater. 2017;105(8):2352-9.

44. Madsen SJ, Christie C, Hong SJ, Trinidad A, Peng Q, Uzal FA, et al. Nanoparticle-loaded macrophage-mediated photothermal therapy: potential for glioma treatment. Lasers in medical science. 2015;30(4):1357-65.

45. Li J, Chen J, Kirsner R. Pathophysiology of acute wound healing. Clinics in dermatology. 2007;25(1):9-18.

46. Kim JH, Song HY, Park JH, Yoon HJ, Park HG, Kim DK. IN-1233, an ALK-5 inhibitor: prevention of granulation tissue formation after bare metallic stent placement in a rat urethral model. Radiology. 2010;255(1):75-82.

47. Diegelmann RF, Evans MC. Wound healing: an overview of acute, fibrotic and delayed healing. Frontiers in bioscience : a journal and virtual library. 2004;9:283-9.

국문요약

배경 및 목적: 스텐트 삽입후 발생되는 조직 과증식 억제를 위한 다양한 스텐트 기술에 대한 발전에도 불구하고, 현재의 치료 전략은 임상적 결과는 아직 충분한 결과를 얻지 못하고 있음. 본 연구의 목적은 백서 위장관 모델에서 비 피복형 스텐트 삽입에 의해 발생되는 조직 과증식을 억제하기 위한 광열 치료의 효능을 평가하고 스텐트가 삽입된 백서 위장관 조직에서 섬유화 억제의 가능성을 입증하고자 함.

연구 방법: 근적외선 레이저 조사 하에 광열치료가 가능한 나노 입자가 코팅된 비 피폭형 자가 팽창형 금속스텐트를 2 단계 합성 과정을 통해 제작하였음. 45 마리의 백서 위장관 모델에서 스텐트를 삽입한 뒤 코팅하지 않은 스텐트를 삽입한 그룹을 제외한 2 그룹을 무작위로 나누었다. 대조군(A 군)은 비 피폭형 스텐트를 삽입한 뒤 근적외선을 조사하지 군이며, 실험군(B 군)은 금 나노 입자가 코팅된 스텐트를 삽입한 뒤 55° C의 국소 열 치료를 진행하였음. 대조군(C 군)은 금 나노 입자가 코팅된 스텐트를 삽입한 뒤 금 나노 입자가 갖는 영향의 유무를 확인하고자 하는 대조군으로 실험을 진행하였음. 국소 열 치료의 치료 효과를 확인하기 위하여 백서 위장관 조직의 단백질발현 분석법 및 조직병리분석을 이용하였음. 단백질발현 분석을 하기 위해, 모든 군에서 각각 5 마리씩 열치료를 한 직후 희생하였음. 단백질발현 분석법에 사용된 항체는 hsp70 이었음. 모든 군에서 남은 10 마리씩 조직병리분석을 위해 스텐트 삽입 후 4 주 후에 희생하였음.

연구 결과: 비 피폭형 금속 스텐트는 2 단계의 합성 과정을 통해 성공적으로 금 나노 입자가 코팅되었음. 스텐트 삽입술 및 국소 열 치료는 모든 백서에서 성공적이었음. 스텐트 삽입으로 유발된 조직 과증식 관련 변수는 A 군과 C 군보다 B 군에서 통계적으로 유의하게 낮았음 ($p < 0.001$). 스텐트 삽입술로 인한 혈관신생의 정도 또한 A 군과 C 군보다 B 군에서 통계적으로 유의하게 낮았음 ($p < 0.001$). 그러나, 열 치료에 의한 조직 괴사는 A 군과 C 군보다 B 군에서 통계적으로 유의하게 높았다 ($p < 0.001$). 조직 증식인자의 형광면역염색 결과의 경우 A 군과 C 군에서 B 군 보다 더 현저히 증식이 많게 나왔음.

연구 결론: 백서 위장관 모델에서 비 피복형 스텐트 삽입 후 발생되는 조직 과증식을 광열치료를 이용하여 효과적으로 억제함을 확인하였음.

(**중심 단어**: 광열치료, 국소 열 치료, 금 나노 입자 스텐트, 조직 과증식, 위장관 폐쇄)